J Mater Sci: Mater Med (2011) 22:2319–2327
DOI 10.1007/s10856-011-4407-3

Mechanical properties and in vivo performance of a novel sliding-lock bioabsorbable poly-*p*-dioxanone stent

Qimao Feng · Wenbo Jiang · Kun Sun · Kang Sun · Sun Chen · Lijiao Zhao · Ke Dai · Ning Ma

Received: 22 April 2011 / Accepted: 28 July 2011 / Published online: 6 August 2011

Abstract A bioabsorbable poly-*p*-dioxanone (PPDO) stent with a novel sliding-lock structure was fabricated to treat stenotic peripheral vessels. The sliding-lock PPDO stents have greater radial strength (107 kPa) than PPDO stents with conventional net-tube structure (32 kPa). The sliding-lock PPDO stents were implanted into the iliac arteries of pigs, and implantation success rate was 90% indicating the feasibility of this design. Additionally, we found that sliding-lock PPDO stents kept vessels patent, although by 3 and 6 months post implantation, luminal diameter decreased slightly due to intimal hyperplasia. At 1 month post implantation, the stents were sparsely covered with endothelial cells, and by 6 months, the stents were mostly absorbed and inflammatory reaction gradually decreased as the stents were absorbed. This study shows favorable mechanical strength, degradability and efficacy for the sliding-lock PPDO stents, and supports further research and development of this unique design of polymer stents for applications in vascular devices.

Q. Feng · K. Sun (✉) · S. Chen · L. Zhao
Children's Heart Center, Xinhua Hospital, Shanghai Jiaotong University School of Medicine, Shanghai 200092, China
e-mail: kunsun@yahoo.cn

W. Jiang · K. Sun
The State Key Laboratory of Metal Matrix Composites, Shanghai Jiaotong University, Shanghai 200240, China

K. Dai · N. Ma
Heart Center, Shanghai Children's Medical Center, Shanghai Jiaotong University School of Medicine, Shanghai 200127, China

1 Introduction

An established treatment for coronary heart disease is percutaneous coronary intervention (PCI) with stent implantation [1, 2]. Recently, attention has been drawn to bioabsorbable stents as they can be safely absorbed by the body without requiring surgical removal and because they might have a lesser potential for late stent thrombosis and chronic inflammation than permanent metallic stents [3–5]. Additional potential advantages of bioabsorbable stents include facilitation of repeat treatments to the same site, restoration of vasomotion and improved lesion imaging with multislice computed tomography (CT) or magnetic resonance imaging (MRI) [3, 6]. Bioabsorbable stents are particularly advantageous for children with vascular stenosis. Permanent metallic stents create a fixed diameter for the stented vessel, and with the growth of the child, the vessel will become stenotic again and require subsequent dilation [7, 8]. However, a bioabsorbable stent could provide short-term scaffolding and would not interfere with vessel growth.

In a previous study, poly-L-lactic acid (PLLA) was selected to make a bioabsorbable stent that is absorbed in vivo through the hydrolysis of bonds between repeating lactide units [3, 9, 10]. The Igaki–Tamai stent, which is made up of PLLA, was initially developed to have a zig-zag helical coil structure with straight bridges [10]. Another bioabsorbable stent, the BVS everolimus-eluting stent, was constructed with a backbone of PLLA and a coating of poly-D,L-lactide containing an anti-proliferate drug and was reported to have clinical and imaging outcomes similar to those of metallic drug-eluting stents for 2 years [3]. However, the degradation time of PLLA (24 months) is somewhat long, especially when these stents are used in growing children. In fact, the stent's role

of mechanical support for the vessel is temporary, lasting only until vascular healing and reendothelialization occurs. Beyond this point, stents provide no advantage and their presence could be a nidus for late thrombosis and chronic inflammation [11–13]. Ormiston and Serruys [14] reviewed the literature on stents for vascular stenosis and indicated that a mechanically intact stent was required to counter negative remodeling and limit restenosis for the first 1–3 months after surgery, and was not needed beyond 6 months. Though several bioabsorbable stents have been developed using magnesium and iron-based alloys [15–17], developing a bioabsorbable stent for the treatment of stenotic vessels with sufficient mechanical properties and appropriate degradation time remains a challenge.

The purpose of this study is to design a new bioabsorbable stent for use in growing children with peripheral vascular stenosis. Bioabsorbable PPDO was selected as the material for the stent over PLLA as its degradation time is faster. Although PPDO has been widely used in absorbable sutures [18], as far as we know, PPDO has never been used for stents to treat stenotic vessels. Here we discuss a stent with a novel sliding-lock structure that improves the mechanical properties of the stent. To evaluate the technical feasibility of these sliding-lock PPDO stents, we implanted them in the iliac arteries of pigs. Further evaluation of the stents' effectiveness and performance was conducted through in vivo studies.

2 Materials and methods

2.1 Materials

PPDO with number-average molecular weight of 2×10^5 was purchased from Johnson & Johnson Medical Ltd. (USA) to fabricate peripheral vascular stents for this study. Two control stents were used in this study: a commercially available stainless steel metal stent (Lifetech Scientific Co. China) and a self-expandable PPDO stent with a net-tube structure that is fabricated by knitting PPDO fibers with a diameter of 0.2 mm into a tubular structure with coverage area of 41% (supplied by Biomaterial Laboratory of Shanghai Jiaotong University, China).

2.2 Design of sliding-lock stents

The PPDO peripheral vascular stent was designed to have a novel sliding-lock structure as shown in Fig. 1. The sliding-lock stent consists of a framework and lamellar mesh structure with small barbs on each side. The lamellar mesh structure is inserted into the frame and coiled to form a tubular stent. The diameter of the stent can be adjusted by sliding the lamellar mesh structure. Hence, the stent can be expanded using a balloon and when the balloon is withdrawn, the barbs on each side of the mesh structure prevent recoil of the stent.

2.3 Fabrication of sliding-lock stents

A micro-jetting manufacture system (MJM) as shown in Fig. 2 was used to fabricate the sliding-lock PPDO stents. Briefly, PPDO was inserted into a stainless steel syringe and heated using a heating band. When the polymer reached the molten phase, PPDO was extruded through a nozzle and deposited on a continuously moving platform controlled by computer. The sliding-lock stent was finally fabricated by depositing PPDO fibers along the predefined path (Fig. 1). Optical images of the fabricated stents are shown in Fig. 3a–c. The width of the struts and the pores between struts is approximately 0.5 mm, and the thickness and coverage area of the sliding-lock stent are approximately 0.2 mm and 41% respectively.

2.4 Mechanical properties

A radial expansion force gage (RX650, Machine Solution Inc, US) was used to measure the radial strength of the sliding-lock PPDO stents. The stainless steel metallic and self-expandable net-tube PPDO control stents (Fig. 3c) were also tested for radial strength. All test stents were put into a chamber kept at a temperature of 37°C, and were compressed along the radial direction at a speed of 0.1 mm/s. Radial strength at various compressed diameters was recorded by a computer, and maximal radial strength was defined as the radial strength when the stent was compressed to 88% of its original diameter [19].

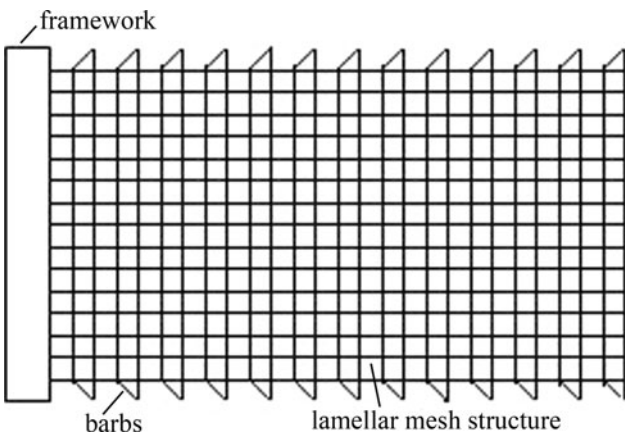

Fig. 1 Schematic illustration of a PPDO stent with the novel sliding-lock structure. The sliding-lock stent consists of a framework and lamellar mesh structure with small barbs on each side

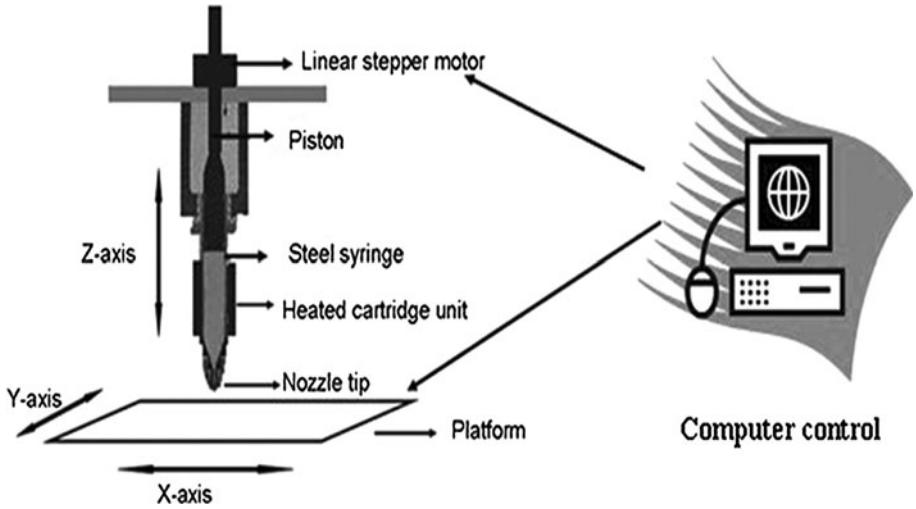

Fig. 2 Schematic illustration of the MJM system. PPDO was inserted into a stainless steel syringe and heated using a heating band. When the polymer reached the molten phase, PPDO was extruded through a nozzle and deposited on a continuously moving platform controlled by computer

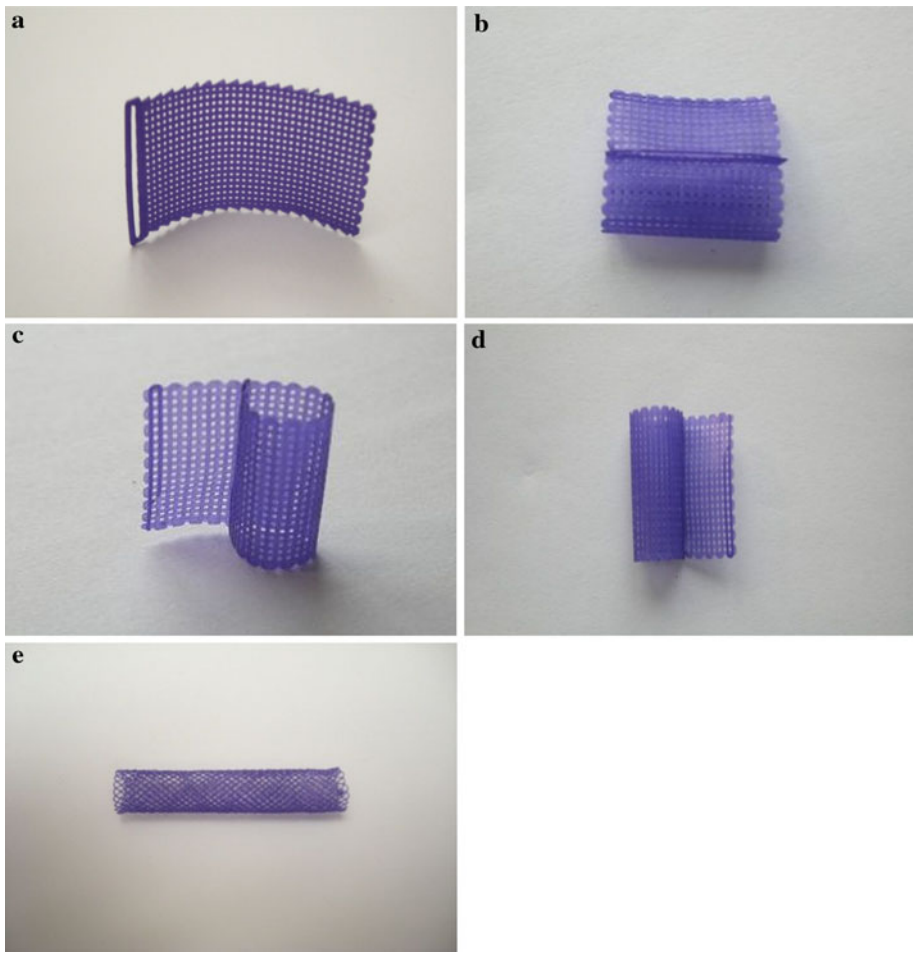

Fig. 3 Photographs of different types of PPDO stents with same thickness of 0.2 mm and same coverage area of 41%. **a** sliding-lock PPDO stent with a lamellar structure; **b–d** The lamellar mesh structure is inserted into the framework and coiled to form a tubular stent, and the barbs on each side of the mesh structure prevent recoil of the stent, and the stent diameter can be adjusted by sliding the lamellar mesh structure; **e** self-expandable net-tube PPDO stent

2.5 Procedure of stent implantation

The study protocol was approved by the local ethical committee for animal care and use. Forty biodegradable sliding-lock PPDO stents of 6-mm diameter, 20-mm length, and 0.2-mm thickness were tested by implantation into the iliac artery of pigs. Pigs ($n = 36$) weighting 18–25 kg were used in this study. A radiopaque marker

was mounted on the PPDO stent and all stents were sterilized by ethylene oxide prior to being mounted on a special stent delivery system.

After each pig was anesthetized, angiography of the iliac arteries was performed to determine target site and the appropriate size for the stent (the ratio of stent diameter to artery diameter was 1.20–1.25:1.0). A special delivery system was used to implant the stent. The stent advanced along either the left or right iliac arteries by following a guide wire fed through the carotid artery using an 8-Fr artery sheath. Once the stent was in position, a balloon was inflated to 14–20 atmospheres for 15–20 s to dilate the artery and allow for the release of the sliding-lock PPDO stent (Fig. 4). A second angiography was performed after implantation to confirm the effectiveness of the stent.

2.6 Performance in vivo

Subsequent angiographies and histological analyses were conducted at 1, 3, and 6 months post implantation. The diameter of each stented vessel was measured to evaluate the efficacy of the sliding-lock PPDO stents in vivo. Sections of the stented vessels with 5-μm thickness were obtained for hematoxylin and eosin (H&E) staining. Neointimal thickness at each stent strut was measured, and sections were imaged at 50× magnification. Cell inflammation and degradability of the PPDO stents were also evaluated. The endothelialization of stented vessels was evaluated using a scanning electron microscope.

2.7 Statistical analysis

All data are presented as mean with standard deviation (mean ± SD). The comparison of radial strength of each stent type was evaluated using one-way analysis of variation, and for the intimal thickness and diameter of the stented vessels at different time, the significances were analyzed using a randomized block design analysis of variance (ANOVA, SPSS, Chicago, IL, USA). P values that were less than 0.05 were considered statistically significant.

3 Results

3.1 Mechanical properties

The radial strength of the different stents is shown in Fig. 5. The commercial stainless steel stent has the highest radial strength of 135.30 ± 5.80 kPa, whereas the radial strength of the PPDO stent with net-tube structure is 32.20 ± 4.30 kPa. However, the PPDO stent with the sliding-lock structure has an intermediate radial strength of 107.50 ± 4.30 kPa. There are statistically significant differences between the three groups ($P < 0.05$).

3.2 Efficacy in vivo

Three pigs died during the procedure: one died due to complications with anesthesia, and two died due to

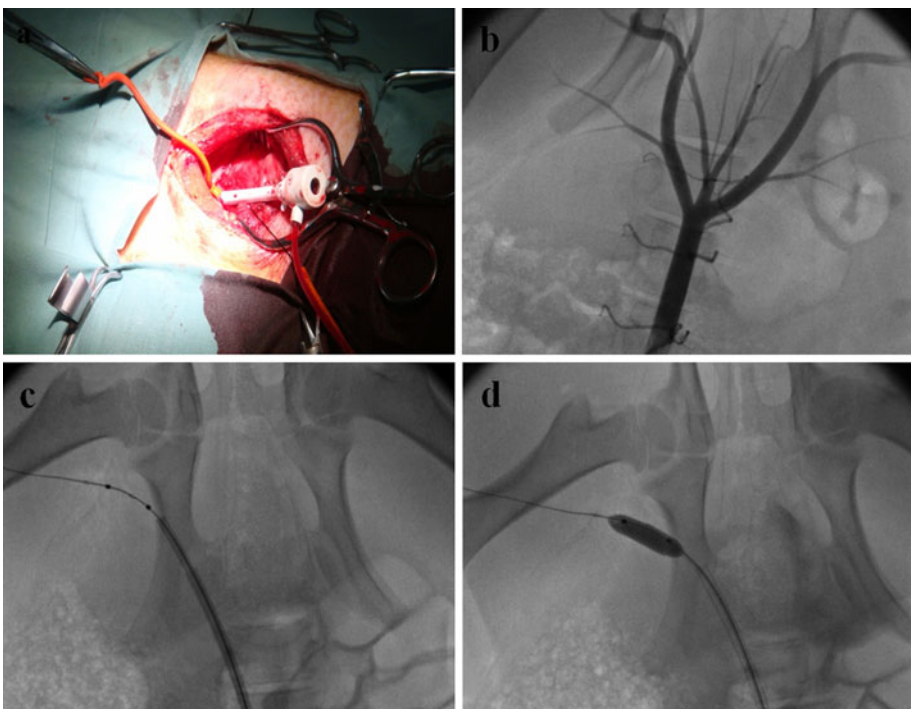

Fig. 4 Sliding-lock PPDO stent implantation procedure. **a** An artery sheath is inserted into the carotid artery; **b** angiography of left and right iliac arteries; **c** the sliding-lock PPDO stent is positioned at target site; **d** the sliding-lock PPDO stent is dilated and released

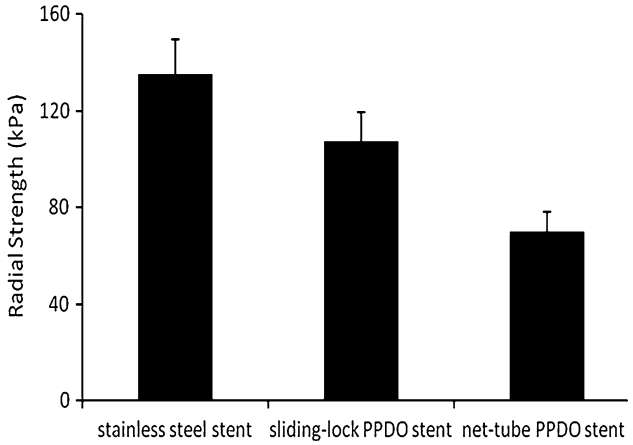

Fig. 5 Average radial strength of each stent type. Averages are based on 10 stents. The radial strength of test stents was measured by a radial expansion force gage

hemorrhoea caused by vessel laceration. Another non-fatal complication involved a stent that did not fully dilate because the balloon ruptured during implantation. The success rate for stent implantation was 90%, while the complication rate was 5%.

Examples of vessel angiograms after stent implantation can be found in Fig. 6, and the average diameters of the stented vessels are shown in Fig. 7. Average vessel diameter 2 min post implantation (5.92 ± 0.06 mm) was not significantly different from the average vessel diameter 1 month post implantation (5.85 ± 0.04 mm) ($P > 0.05$). However, the average vessel diameter at both 3 months (4.86 ± 0.09 mm) and 6 months (4.84 ± 0.11 mm) post implantation were significantly smaller than that 1 month after implantation ($P < 0.05$). Figure 8 illustrates that intimal thickness at 3 (0.31 ± 0.04 mm) and 6 (0.32 ± 0.05 mm) months post implantation was much greater than that 1 month after surgery (0.18 ± 0.02 mm) ($P < 0.05$).

3.3 Biodegradability and biocompatibility

Histological examinations were conducted to evaluate the biodegradable and biocompatible properties of PPDO stents and the results are shown in Fig. 9. One month post implantation the struts of the PPDO stents are still integrated and barely degraded. However, by 3 months post implantation, the struts have been partly degraded, and 6 months after implantation, the struts are mostly absorbed and what remains has been degraded into pieces. A few inflammatory cells including leukomonocytes, plasmocytes, and eosinophil granulocytes, began to aggregate

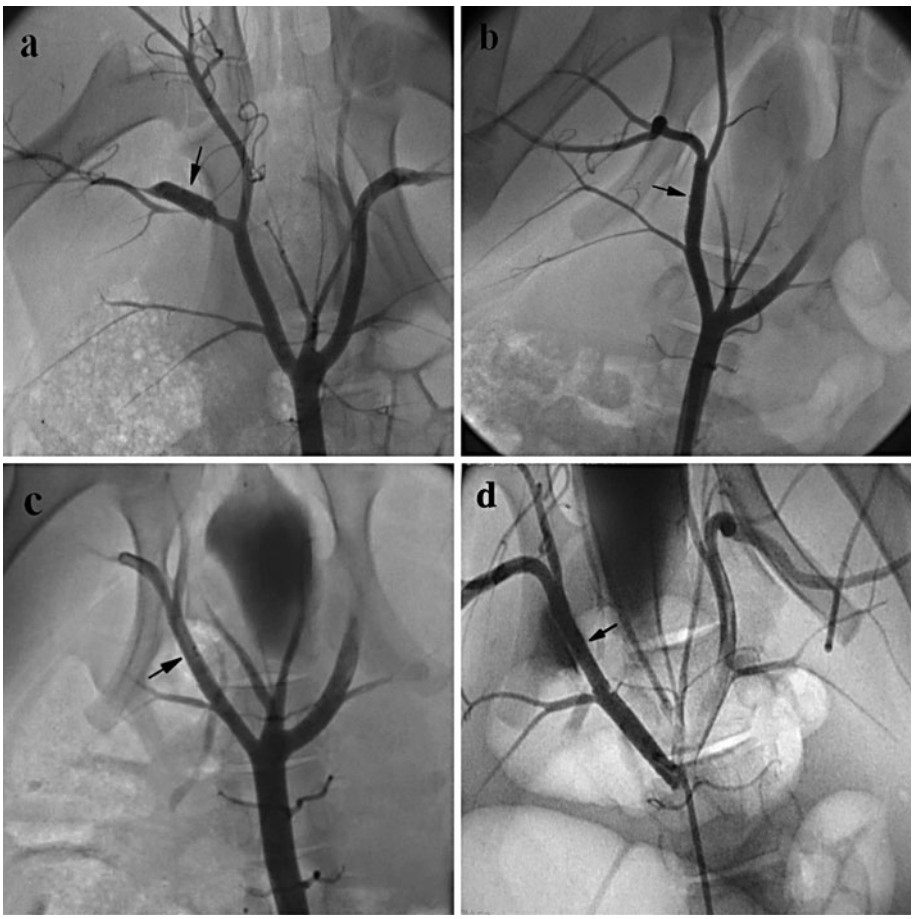

Fig. 6 Angiography of the stented vessels at different times after implantation. **a** At 2 min post implantation, the vessels at each end of the stent become spastic; **b** at 1 month post implantation, the stented vessel remains patent; **c**, **d** at 3 (**c**) and 6 (**d**) months post implantation, the stented vessels keep patent well, although their diameter lost a little

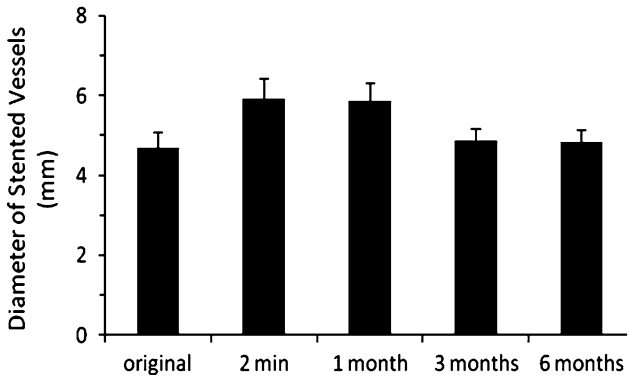

Fig. 7 Average diameter of the stented vessels at before implantation, 2 min, 1, 3 and 6 months post implantation, and averages are based on nine stents. The luminal diameter was measured by quantitative angiography

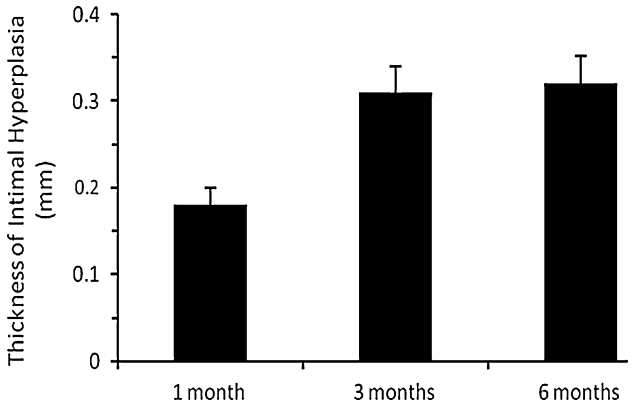

Fig. 8 Average thickness of intimal hyperplasia at 1, 3 and 6 months after stent implantation, and averages are based on nine stents. The intimal thickness was measured for hematoxylin- and eosin-stained cross sections under a light microscope

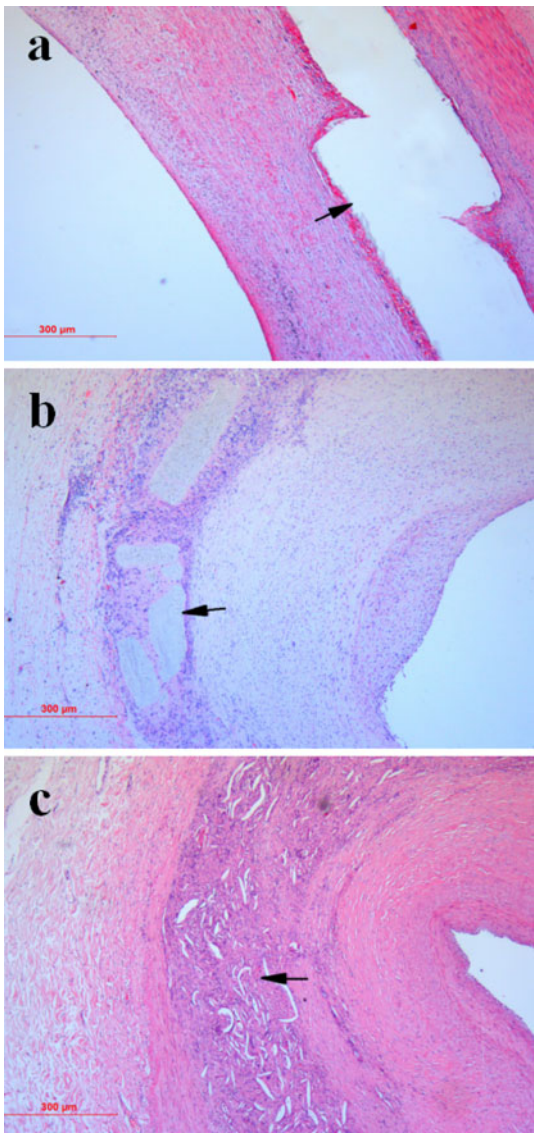

Fig. 9 Light microscopy of pig iliac arteries harvested at different times after stent implantation. At all points post implantation, there is evidence of some inflammatory reaction in the arterial wall. Notably, smooth muscle cell necrosis was not observed. A thin to moderate neointima that mostly consisted of smooth muscle cells and fibroblasts was formed in response to PPDO stents. **a** PPDO stents have been covered by intima and struts are barely degraded 1 month after implantation, and the partial overlap of the stent was showed; **b** 3 months post implantation, several inflammatory cells have aggregated around the struts and stents are more highly degraded. **c** At 6 months post implantation, the inflammatory reaction has lessened as the stent materials have been mostly absorbed

around the struts 1 month after implantation. At 3 months post implantation, many inflammatory cells aggregated around the struts, but the inflammatory reaction gradually lessened with time as stent materials were mostly absorbed 6 months post implantation. One month post implantation, there is a sparse covering of endothelial cells around the PPDO stents, but by 3 and 6 months post surgery, the PPDO stents are compactly covered with endothelial cells and this covering forms a new endomembrane (Fig. 10).

4 Discussion

A novel PPDO stent with a sliding-lock structure was developed for the treatment of stenotic vessels. The sliding-lock stents are fabricated with a lamellar structure and they use their own barbs to form circular stents. Whereas traditional vascular stents are generally tubular in shape and either open or close cells depending on the requirements of the vascular lesion [20, 21]. The advantages of the sliding-lock PPDA stent are that its radial strength can be greatly increased (Fig. 5), and its diameter can be easily adjusted through the sliding of the lamellar mesh structure. The unique structure of sliding-lock stent differs from the REVA Bioabsorbable Stent, made of a tyrosine-derived

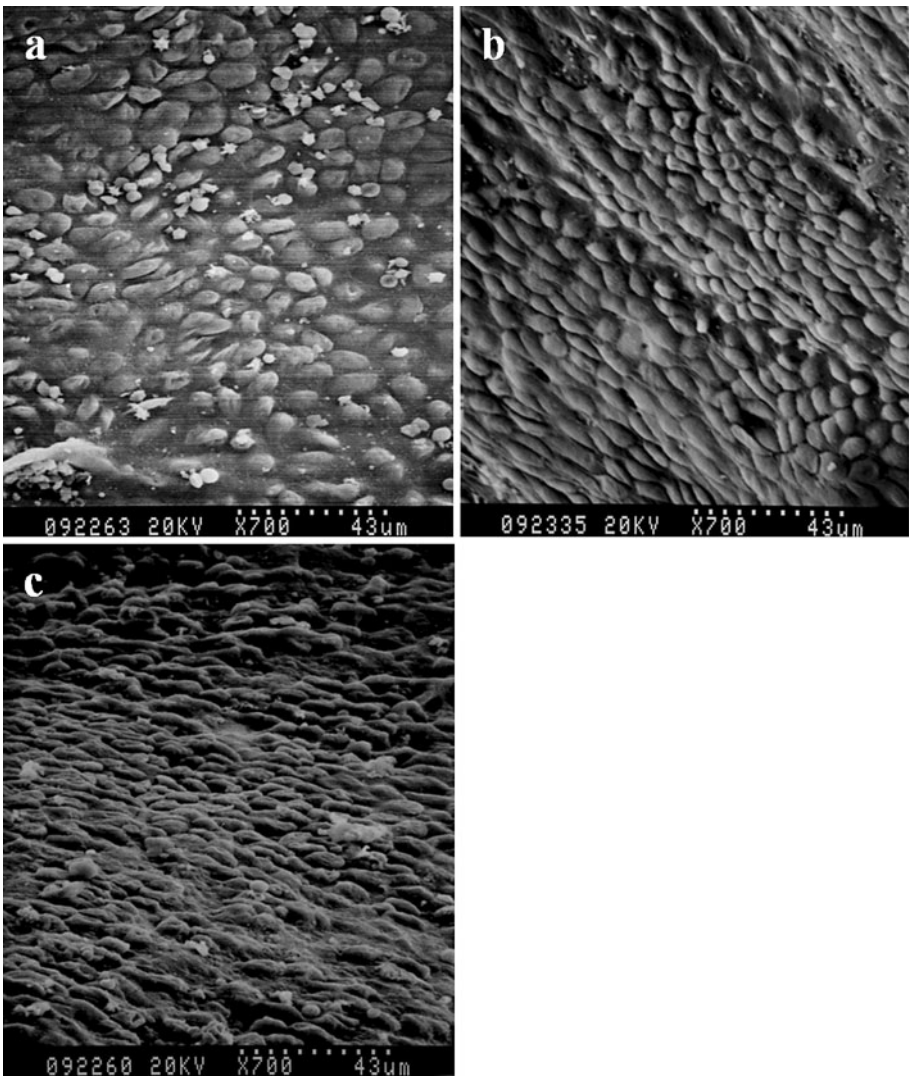

Fig. 10 Scanning electron microscope images of pig iliac arteries harvested at different times after stent implantation. **a** At 1 month post implantation, the stented vessels are sparsely covered by endothelial cells; **b**, **c** at 3 (**b**) and 6 (**c**) months post implantation, endothelial cells form a compact intimal covering

polycarbonate developed at Rutgers University and consisting of three independent lamellas that connect and slide each other, and the growth stent that comprises of two separate halves of the metal stent connected in the middle by absorbable suture [22].

The PPDO stents were prepared using a MJM system. This process is very flexible because the size of the pores and barbs and the thickness of the stents can be easily adjusted using a computer. Therefore, this preparation technique may provide an ideal way for design and preparation of individual drug-eluting stents, which can accomplish drug homogeneous distribution or drug concentration gradient in the stents.

Radial strength is a key predictor of the effectiveness of stents in vivo. Radial strength should be above 80–120 kPa to meet clinical requirements for peripheral vascular stents [23]. Self-expandable net-tube PPDO stents have an average radial strength of only 32.2 kPa because of its slightly loose structure, which fails to meet the clinical requirements for peripheral vascular stents. However, the average radial strength of sliding-lock PPDO stents is 107 kPa, which is still somewhat lower than that of commercial stainless steel stents (135 kPa) but well within the clinically useful range of 80–120 kPa. Therefore, sliding-lock PPDO stents satisfy the clinical requirements for radial strength for the treatment of stenotic peripheral vessels.

The technical feasibility of sliding-lock PPDO stents was evaluated by implantation into the iliac arteries of pigs where their effectiveness and performance could be studied in vivo. Our results indicate that, 1 month post implantation, the diameter of the stented vessel remains patent, maintaining nearly the same diameter as measured 2 min post implantation. Nevertheless, 3 months post implantation, the vascular diameter decreases by approximately 18% (from 5.92 to 4.86 mm), and this decreased diameter is likely due to intimal hyperplasia. Vessel diameter changes minimally between 3 and 6 months after surgery,

indicating that after 3 months, the diameter of the stented vessel is stable and that further stenosis is unlikely.

Intimal hyperplasia occurred after stent implantation resulting from stress and injury to the vessel wall and from the subsequent inflammatory reaction [24, 25]. As shown in Fig. 8, intimal thickness increased from 0.18 mm at 1 month post surgery to 0.31 mm at 3 months post implantation. This increase in intimal thickness may be due to the inflammatory reaction as well as the biodegradation of the PPDO stents as shown in Fig. 9b. The ratio of stent diameter to vessel diameter (1.20–1.25:1.0) used in this study is a bit higher than that used in other studies [15, 16, 26]. A greater stent diameter-to-vessel diameter ratio leads to greater stress and injury to vessel walls that promote intimal hyperplasia. As with vessel diameter, there was no significant change in intimal thickness between 3 and 6 months post implantation. Potential explanations for this lack of change in intimal thickness may be that the injured vessel walls have recovered, the stress in the vessel walls has disappeared, or that the inflammatory reaction around the struts decreased as the PPDO stents degraded.

As a bioabsorbable stent for growing children, it is important that the rate of stent degradation match the rate of vascular remodeling and vessel growth. Iron stents degrade too slowly [16, 17], but magnesium stents that have been implanted into the coronary arteries of pigs have been found to degrade too quickly, leading to negative remodeling [15]. However, Zartner et al. [27, 28] implanted a magnesium stent in the left pulmonary artery of a premature infant and reported that the stented vascular diameter increased from 3.0 to 3.7 mm, 5 months post implantation. These results indicate that in children a stent may only be required for 1–2 months. We found that the struts of the PPDO stents started to degrade 3 months post implantation and were mostly absorbed at 6 months post surgery (Fig. 9), which suggested that PPDO stents kept their mechanical role for at least 2 months and are more biodegradable than PLLA stents (mostly absorbed by 24 months).

The local inflammatory reaction is often used to evaluate the biocompatibility of biomaterials in vivo [29]. PPDO was reported to have good biocompatibility and has been used widely to make sutures for cardiac surgery [18]. Results from this study illustrated in Fig. 9 suggest that PPDO stents cause a strong inflammatory response with many inflammatory cells aggregating around the struts at 3 months post implantation. Potential explanations for this may be that PPDO stents have started to degrade into lots of pieces at 3 months post surgery, and as a foreign body, those degradable materials bring about strong host response [29, 30]. Zamiri et al. [31] has reported that PPDO, woven into a braided structure and secured to bare metal stents and together implanted into porcine carotid arteries, was also associated with moderate inflammatory response at 90 days after implantation. However, this inflammatory response is gradually mitigated by 6 months post surgery in this study, which is due to that the struts have been largely absorbed in vivo. The inflammation response of absorbable polymeric materials has been the subject of extensive study [9, 31]. The reduction in inflammation has been reported with everolimus eluting biodegradable PLA stents in the porcine and human coronary arteries [3]. In next study, the drug-eluting PPDO stents may be searched to diminish inflammatory reaction in vivo.

Additionally, endothelialization of stented vessels has been closely associated with cell compatibility of biomaterials in vivo [32, 33]. Figure 10 illustrates PPDO stents covered by endothelial cells 1 month post implantation, and by 3 and 6 months post surgery, the endothelial cell covering becomes denser, suggesting that PPDO has a good cell-compatibility.

5 Conclusions

This study shows favorable mechanical strength, vascular compatibility, degradability and efficacy for the novel sliding-lock PPDO stents, and supports further research and development of this unique design of polymer stents for applications in vascular devices.

Acknowledgments We thank Ruidong Zhang, Zuming Jiang, Xiaoqing Yu, and Yiwei Chen, from the Heart Center, Shanghai Children's Medical Center, Shanghai Jiaotong University School of Medicine, China, for their excellent technical assistance. This work was supported by grants from the National Natural Science Foundation of China (No. 30772349), Science and Technology Commission of Shanghai Municipality, China (No. 07XD14015), and Shanghai Shenkang Hospital Development Center, China (No. SHDC12007107).

References

1. Claessen BE, Mehran R, Leon MB, Heller EA, Weisz G, Syros G, Mintz GS, Franklin-Bond T, Apostolidou I, Henriques JP, Stone GW, Moses JW, Dangas GD. Two-year safety and effectiveness of sirolimus-eluting stents (from a prospective registry). Am J Cardiol. 2011;107(4):528–34.
2. Millauer N, Jüni P, Hofmann A, Wandel S, Bhambhani A, Billinger M, Urwyler N, Wenaweser P, Hellige G, Räber L, Cook S, Vogel R, Togni M, Seiler C, Meier B, Windecker S. Sirolimus versus paclitaxel coronary stents in clinical practice. Catheter Cardiovasc Interv. 2011;77(1):5–12.
3. Serruys PW, Ormiston JA, Onuma Y, Regar E, Gonzalo N, Garcia-Garcia HM, Nieman K, Bruining N, Dorange C, Miquel-Hébert K, Veldhof S, Webster M, Thuesen L, Dudek D. A bioabsorbable everolimus-eluting coronary stent system (ABSORB): 2-year outcomes and results from multiple imaging methods. Lancet. 2009;373(9667):897–910.
4. Waksman R, Erbel R, Di Mario C, Bartunek J, de Bruyne B, Eberli FR, Erne P, Haude M, Horrigan M, Ilsley C, Böse D,

Bonnier H, Koolen J, Lüscher TF, Weissman NJ. Early- and long-term intravascular ultrasound and angiographic findings after bioabsorbable magnesium stent implantation in human coronary arteries. JACC Cardiovasc Interv. 2009;2(4):312–20.
5. Hermawan H, Purnama A, Dube D, Couet J, Mantovani D. Fe–Mn alloys for metallic biodegradable stents: degradation and cell viability studies. Acta Biomater. 2010;6(5):1852–60.
6. Ghimire G, Spiro J, Kharbanda R, Roughton M, Barlis P, Mason M, Ilsley C, Di Mario C, Erbel R, Waksman R, Dalby M. Initial evidence for the return of coronary vasoreactivity following the absorption of bioabsorbable magnesium alloy coronary stents. EuroIntervention. 2009;4(4):481–4.
7. Zanjani KS, Sabi T, Moysich A, Ovroutski S, Peters B, Miera O, Kühne T, Nagdyman N, Berger F, Ewert P. Feasibility and efficacy of stent redilatation in aortic coarctation. Catheter Cardiovasc Interv. 2008;72(4):552–6.
8. Tomita H, Nakanishi T, Hamaoka K, Kobayashi T, Ono Y. Stenting in congenital heart disease: medium- and long-term outcomes from the JPIC stent survey. Circ J. 2010;74(8):1676–83.
9. Vogt F, Stein A, Rettemeier G, Krott N, Hoffmann R, vom Dahl J, Bosserhoff AK, Michaeli W, Hanrath P, Weber C, Blindt R. Long-term assessment of a novel biodegradable paclitaxel-eluting coronary poly-lactide stent. Eur Heart J. 2004;25(15):1330–40.
10. Tamai H, Igaki K, Kyo E, Kosuga K, Kawashima A, Matsui S, Komori H, Tsuji T, Motohara S, Uehata H. Initial and 6-month results of biodegradable poly-L-lactic acid coronary stents in humans. Circulation. 2000;102(4):399–404.
11. Nakazawa G, Finn AV, Vorpahl M, Ladich ER, Kolodgie FD, Virmani R. Coronary responses and differential mechanisms of late stent thrombosis attributed to first-generation sirolimus- and paclitaxel-eluting stents. J Am Coll Cardiol. 2011;57(4):390–8.
12. Niccoli G, Montone RA, Ferrante G, Crea F. The evolving role of inflammatory biomarkers in risk assessment after stent implantation. J Am Coll Cardiol. 2010;56(22):1783–93.
13. Ielasi A, Al-Lamee R, Colombo A. Stent thrombosis and duration of dual antiplatelet therapy. Curr Pharm Des. 2010;16(36):4052–63.
14. Ormiston JA, Serruys PW. Bioabsorbable coronary stents. Circ Cardiovasc Interv. 2009;2(3):255–60.
15. Maeng M, Jensen LO, Falk E, Andersen HR, Thuesen L. Negative vascular remodelling after implantation of bioabsorbable magnesium alloy stents in porcine coronary arteries: a randomised comparison with bare-metal and sirolimus-eluting stents. Heart. 2009;95(3):241–6.
16. Waksman R, Pakala R, Baffour R, Seabron R, Hellinga D, Tio FO. Short-term effects of biocorrodible iron stents in porcine coronary arteries. J Interv Cardiol. 2008;21(1):15–20.
17. Peuster M, Hesse C, Schloo T, Fink C, Beerbaum P, von Schnakenburg C. Long-term biocompatibility of a corrodible peripheral iron stent in the porcine descending aorta. Biomaterials. 2006;27(28):4955–62.
18. Lerwick E. Studies on the efficacy and safety of polydioxanone monofilament absorbable suture. Surg Gynecol Obstet. 1983;156(1):51–5.
19. Tokuda T, Shomura Y, Tanigawa N, Kariya S, Komemushi A, Kojima H, Sawada S. Mechanical characteristics of composite knitted stents. Cardiovasc Interv Radiol. 2009;32(5):1028–32.
20. Stoeckel D, Bonsignore C, Duda S. A survey of stent designs. Minim Invasive Thera Allied Technol. 2002;11(4):137–47.
21. Claessen BE, Caixeta A, Henriques JP, Piek JJ. Current status of the Xience V® everolimus-eluting coronary stent system. Expert Rev Cardiovasc Ther. 2010;8(10):1363–74.
22. Ewert P, Riesenkampff E, Neuss M, Kretschmar O, Nagdyman N, Lange PE. Novel growth stent for the permanent treatment of vessel stenosis in growing children: an experimental study. Catheter Cardiovasc Interv. 2004;62(4):506–10.
23. Schmidt W, Andresen R, Behrens P, Schmitz KP. Characteristic mechanical properties of balloon-expandable peripheral stent systems. Rofo. 2002;174(11):1430–7.
24. Kibos A, Campeanu A, Tintoiu I. Pathophysiology of coronary artery in-stent restenosis. Acute Card Care. 2007;9(2):111–9.
25. Inoue T, Node K. Molecular basis of restenosis and novel issues of drug-eluting stents. Circ J. 2009;73(4):615–21.
26. Jabara R, Chronos N, Robinson K. Novel bioabsorbable salicylate-based polymer as a drug-eluting stent coating. Catheter Cardiovasc Interv. 2008;72(2):186–94.
27. Zartner P, Cesnjevar R, Singer H, Weyand M. First successful implantation of a biodegradable metal stent into the left pulmonary artery of a preterm baby. Catheter Cardiovasc Interv. 2005;66(4):590–4.
28. Zartner P, Buettner M, Singer H, Sigler M. First biodegradable metal stent in a child with congenital heart disease: evaluation of macro and histopathology. Catheter Cardiovasc Interv. 2007;69(3):443–6.
29. Uurto I, Mikkonen J, Parkkinen J, Keski-Nisula L, Nevalainen T, Kellomäki M, Törmälä P, Salenius JP. Drug-eluting biodegradable poly-D/L-lactic acid vascular stents: an experimental pilot study. J Endovasc Ther. 2005;12(3):371–9.
30. Venkatraman S, Boey F, Lao LL. Implanted cardiovascular polymers: natural, synthetic and bio-inspired. Prog Polym Sci. 2008;33(9):853–74.
31. Zamiri P, Kuang Y, Sharma U, Ng TF, Busold RH, Rago AP, Core LA, Palasis M. The biocompatibility of rapidly degrading polymeric stents in porcine carotid arteries. Biomaterials. 2010;31(31):7847–55.
32. Pendyala LK, Yin X, Li J, Chen JP, Chronos N, Hou D. The first-generation drug-eluting stents and coronary endothelial dysfunction. JACC Cardiovasc Interv. 2009;2(12):1169–77.
33. Yao ZH, Matsubara T, Inada T, Suzuki Y, Suzuki T. Neointimal coverage of sirolimus-eluting stents 6 months and 12 months after implantation: evaluation by optical coherence tomography. Chin Med J (Engl). 2008;121(6):503–7.